Bull. Mater. Sci., Vol. 34, No. 7, December 2011, pp. 1421–1434. © Indian Academy of Sciences.

Effect of thermomechanical processing on evolution of various phases in Ti–Nb alloys

S BANUMATHY, K S PRASAD, R K MANDAL[†] and A K SINGH*

Defence Metallurgical Research Laboratory, Kanchanbagh P.O., Hyderabad 500 058, India
[†]Department of Metallurgical Engineering, Institute of Technology, Banaras Hindu University, Varanasi 221 005, India

MS received 28 April 2010; revised 2 November 2010

Abstract. **This paper deals with the effect of thermomechanical processing on microstructural evolution of three alloys, viz. Ti–8Nb, Ti–12Nb and Ti–16Nb. The alloys were hot rolled at 800°C and then subjected to various heat treatments. Samples from hot-rolled alloys were given solution-treatment in β and $\alpha+\beta$ phase fields, respectively followed by water quenching and furnace cooling. The solution-treated alloys were subsequently aged at different temperatures for 24 h. Phases evolved after various heat treatments were studied using X-ray diffractometer, optical, scanning and transmission electron microscopes. The alloy Ti–8Nb exhibits α and β phases while the alloys Ti–12Nb and Ti–16Nb show the presence of α'', β and ω phases in the as-cast and hot-rolled conditions. The β solution treated and water quenched specimen of the alloy Ti–8Nb displays α'' phase while the alloys Ti–12Nb and Ti–16Nb exhibit α'', β and ω phases. The alloy Ti–8Nb shows the presence of α, β and ω phases while those of Ti–12Nb and Ti–16Nb display the presence of α, α'', β and ω in $\alpha+\beta$ solution treated and water quenched condition. The observation of ω phase in solution treated condition depends on the cooling rate and the Nb content while in the aged specimens, it is governed by aging temperature as well as the Nb content.**

Keywords. **Heat treatment; Ti–Nb alloys; thermomechanical processing; microstructure; X-ray diffraction.**

1. Introduction

Titanium and its alloys, owing to their attractive properties are widely used in aerospace applications (Collings 1984; Boyer *et al* 1994). Efforts over the last four decades have resulted in the development of excellent conventional alloys for application in temperature range between 420 K (replacing aluminum alloys) and 875 K (in place of super alloys). In addition, titanium alloys are also widely used as implants in orthopedics, dentistry and cardiology due to their outstanding biomedical compatibility. Eylon *et al* (1984) reviewed various aspects of development of these alloys. These are grouped into five classes viz. α, near α, $\alpha+\beta$, near β and β depending on the concentration of α and β stabilizing elements.

The Ti–Nb binary alloys have been extensively studied as they exhibit several equilibrium and non-equilibrium phases depending on the composition and heat treatments (Collings 1984; Boyer *et al* 1994). Murray (1987) has given an assessed equilibrium binary phase diagram of Ti–Nb. A schematic representation of the occurrence of metastable phases such as α', α'' and ω for the Ti-transition metal system and related phase field as function of temperature and *e*/*a* ratio is shown elsewhere (Collings 1984; Boyer *et al* 1994). Although different types of phase transformations involving the occurrence of equilibrium and non-equilibrium phases have been reported in Ti–Nb alloys in the range of 0–20-atom% Nb, a systematic study on the effect of thermomechanical processing on evolution of various phases appears to be lacking in the literature. This includes investigation pertaining to competing phase transformations between $\beta \rightarrow$ martensite (α' and α'') and $\beta \rightarrow \omega$, cooling rate dependence of transformation products as well as the effect of aging temperature.

The Ti–Nb alloys are most widely used as superconducting materials and also find uses in aerospace applications (Collings 1984; Boyer *et al* 1994). It is important that the relative phase stability in this system is understood properly. It is well known that the evolution of microstructure and phases in titanium alloys can be controlled by thermomechanical treatment. This investigation is thus undertaken to study the effects of mechanical working and heat treatment on the evolution of structures and microstructures in Ti–8Nb, Ti–12Nb and Ti–16Nb alloys. The Nb concentrations in the present alloys are greater than the critical limit of α'/α'' transition after β solution treatment and water quenching. The Nb is a well known β stabilizer and the presence of β phase in the microstructure

*Author for correspondence (singh_ashok3@rediffmail.com)

Table 1. Chemical composition of experimental alloys.

Alloy	Ti (atom %)	Nb (atom %)	Interstitial contents (ppm)		
			Oxygen	Nitrogen	Hydrogen
Ti–8Nb	91·7	8·3	1150	47	20
Ti–12Nb	87·9	12·1	1197	54	22
Ti–16Nb	83·6	16·4	1010	63	26

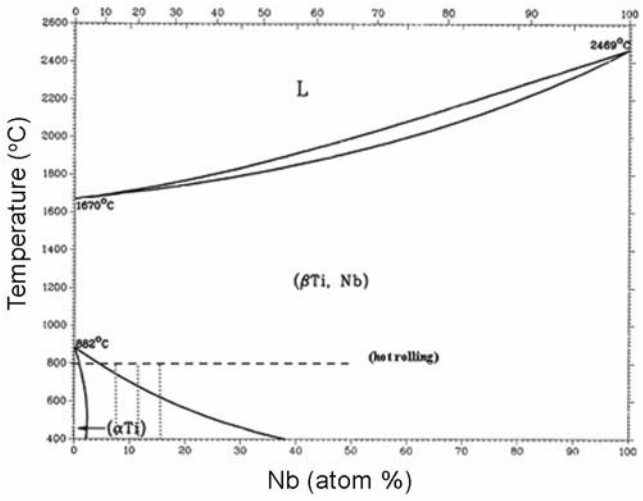

Figure 1. Equilibrium binary phase diagram of Ti–Nb system (Murray 1987).

enhances the ability of alloy to harden on subsequent aging (Collings 1984; Boyer *et al* 1994).

2. Experimental

2.1 *Alloy preparation*

Six hundred grams of pancakes of three alloys, Ti–8Nb, Ti–12Nb and Ti–16Nb were prepared by non-consumable vacuum arc melting technique and melting was repeated six times to ensure chemical homogeneity. The analysed compositions of the cast alloys are given in table 1. The pancakes were, thereafter, subjected to unidirectional hot rolling in the β phase field (800°C) to 80% reduction and air cooled (AC). The reduction in each pass was around 5%. The equilibrium binary phase diagram of Ti–Nb system is shown in figure 1. The β transus temperature obtained by differential scanning calorimetry (DSC) for Ti–8Nb, Ti–12Nb and Ti–16Nb were 785 ± 5°C, 740 ± 5°C and 690 ± 5°C, respectively which are in agreement with the equilibrium binary phase diagram (figure 1). Small samples of size 20 mm × 15 mm × 3 mm were cut from the rolled alloys for solution treatment (ST) studies. The solution treatments consisted of a high temperature (β ST) and low temperature ($\alpha + \beta$ ST) followed by water quenching (WQ) and furnace cooling (FC). The WQ specimens were aged at three different temperatures, viz. 350, 450 and 550°C for 24 h and AC.

2.2 *Microstructure and phase analysis*

The specimens for optical and scanning electron microscopy (OM and SEM) were prepared following standard metallographic techniques used for titanium and its alloys and etched with Kroll's reagent (5 ml HF, 10 ml HNO_3 and 85 ml H_2O). The samples were examined in optical microscope in etched condition while in scanning electron microscopy (Leo 440i) in unetched condition in back scattered electron (BSE) mode. Transmission electron microscopy (TEM) of selected samples was carried out using Technaii 2020 transmission electron microscope. The X-ray diffraction (XRD) studies of bulk samples were performed using a Philips 3020 diffractometer with Cu$K\alpha$ radiation. The lattice parameters of the constituent phases in as-cast, hot-rolled and heat-treated specimens were calculated using standard programme Celn (Lagaree 1989–1993). The error in lattice parameters is shown in parenthesis. The electron probe microanalyser (EPMA) was employed to obtain chemical profile of the alloying elements (model: SX100, Ms Cameca). The spectral resolution was around 0·2 μm.

3. Results and discussion

In this §, the microstructures and corresponding XRD results of as-cast, hot-rolled and heat-treated specimens will be discussed in detail. The results will be presented following the above sequence.

3.1 *As-cast alloys*

The optical microstructures of all the alloys reveal prior β grains having very fine mixture of two phases (figure 2). The Ti–12Nb, in addition also reveals the presence of subgrain boundaries. All the alloys display a typical transformed microstructure. The Ti–8Nb alloy reveals the presence of α and β phases while the alloy Ti–12Nb shows α'' (orthorhombic) and β phases (figure 3). XRD pattern of the alloy Ti–16Nb displays the presence of α'' phase only (figure 3). In addition to this, it also exhibits the presence of strong solidification texture in the cast

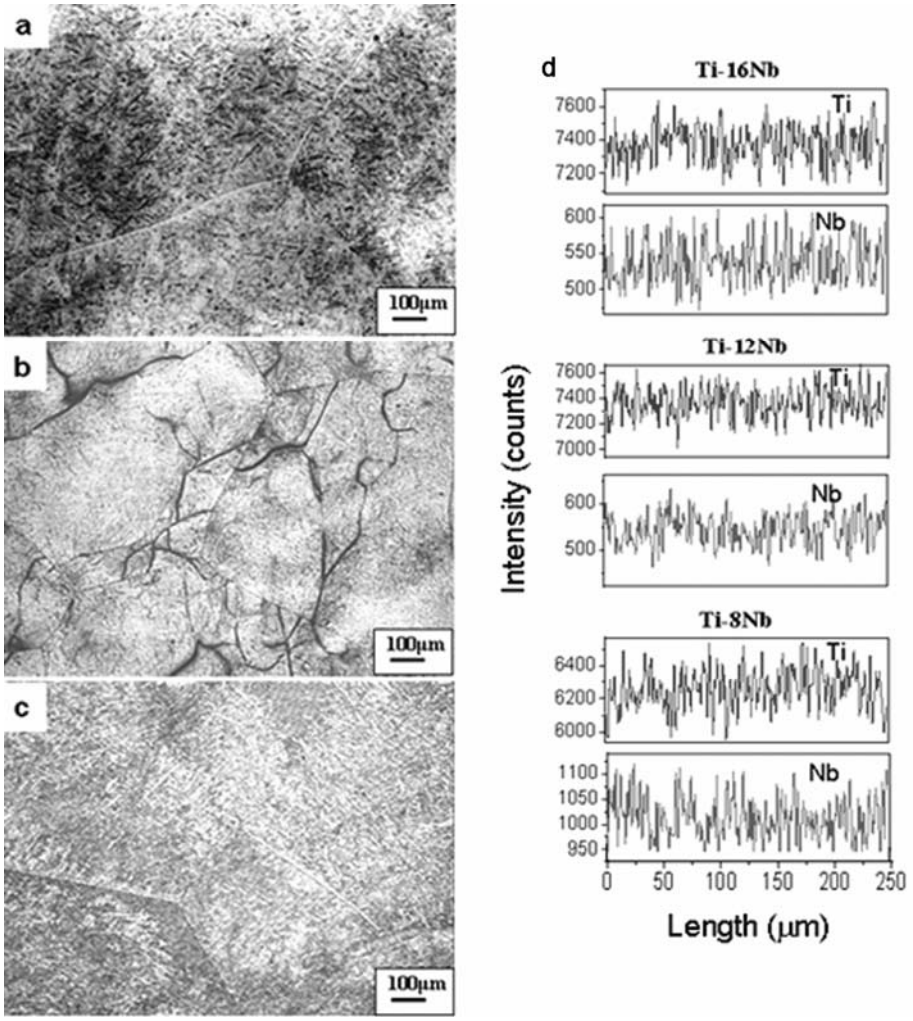

Figure 2. Optical microstructures of as-cast alloys: (**a**) Ti–8Nb, (**b**) Ti–12Nb, (**c**) Ti–16Nb and (**d**) elemental profile of Ti and Nb.

Table 2. Phases observed by XRD and their lattice constants in experimental alloys in as-cast condition.

		Lattice constant (Å)		
Alloy	Phase(s)	*a*	*b*	*c*
Ti–8Nb	α	2·944(6)	–	4·672(6)
	β	3·261(3)	–	–
Ti–12Nb	α''	3·048(4)	5·082(6)	4·639(0)
	β	3·255(6)	–	–
Ti–16Nb	α''	3·170(1)	5·036(0)	4·643(4)

material which can be seen from the strong (310) reflection of the α'' phase. As a result, β phase peaks are getting masked in XRD pattern although the BSE microstructure (not shown) reveals the presence of two phases. The lattice parameters of the corresponding phases are shown in table 2.

Based on the microstructures of the as-cast alloys and XRD patterns, it appears that the alloys first solidify in the single β phase field. The alloy Ti–8Nb then passes to the $\alpha+\beta$ phase field due to solid-state phase transformation, which is stable until room temperature. In the case of alloys, Ti–12Nb and Ti–16Nb, β phase transforms to the $\alpha''+\beta$ phases which seem to be stable until room temperature. The extent of micro segregation is reasonably less (figure 1d) as compared to typical cast materials since these alloys pass through single phase field during solidification.

3.2 *Hot-rolled alloys*

The optical microstructures taken from rolling direction (RD) plane of the hot-rolled specimens demonstrate typical features of rolled microstructures (figure 4). They exhibit elongated prior β grain boundaries consisting of a fine distribution of the constituent phases. The alloy

Ti–8Nb shows an unrecrystallized microstructure while the alloys Ti–12Nb and Ti–16Nb consist of unrecrystallized and recrystallized regions. The volume fractions of recrystallized grains of Ti–12Nb and Ti–16Nb in hot-rolled condition are 22% and 53%, respectively. The extent of recrystallization increases with increase in Nb content. This can be attributed to the high concentration of Nb, which decreases the β transus temperature. As a result, high Nb containing alloys get superheated during hot rolling since the gap between rolling temperature and β transus temperature increases and thereby the alloy Ti–16Nb exhibits the highest volume fraction of recrystallized grains. XRD studies confirm the presence of two phases, α and β, in Ti–8Nb and α'' and β in Ti–12Nb and Ti–16Nb alloys (figure 5). The lattice parameters corresponding to these phases are given in table 3. TEM study of the hot-rolled Ti–16Nb alloy displays fine structure (figure 6a). A composite selected area diffraction (SAD) pattern of β and ω phases is shown in figure 6b.

It is to be noted that the α'' phase has been observed in both the as-cast and hot-rolled conditions in Ti–12Nb and Ti–16Nb. In general, the $\beta \rightarrow \alpha''$ is a martensitic transformation, which has been reported in titanium alloys after β heat treatment and WQ (Brown *et al* 1964; Young *et al* 1974; Sugimoto *et al* 1980; Singh *et al* 1993; Geetha *et al* 2001, 2004). The influence of solute concentration on the kinetics of $\beta \rightarrow \alpha''$ transformation has been studied by Jepson *et al* (1970) on a series of Ti–Nb alloys. It has been shown that martensitic start transformation temperature (M_s) depends on the critical cooling rate (r_c), which decreases with increase in Nb concentration. The critical cooling rate, r_c, for unalloyed Ti is 10^2°C/s and it reduces to 0·3°C/s after addition of 15 atom% Nb (Jepson *et al* 1970). The observation of α'' phase in as-cast and hot-rolled condition of the present study in Ti–12Nb and Ti–16Nb alloys can, therefore, be attributed to high Nb content which reduces critical cooling rate of $\beta \rightarrow \alpha''$ transformation.

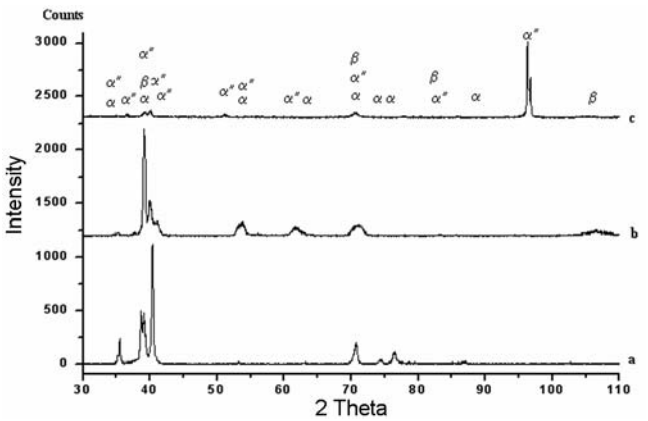

Figure 3. XRD patterns of as-cast alloys: (a) Ti–8Nb, (b) Ti–12Nb and (c) Ti–16Nb.

3.3 *Microstructural features of heat-treated alloys*

3.3a *β heat treatments*: All the alloys in the hot-rolled condition were heat treated above the β transus temperature at 950°C for 30 min (β ST) and cooled at different rates (WQ and FC). This treatment results in various phases depending on alloy composition and cooling rates. The details of heat treatments and phases evolved during cooling are given in table 4.

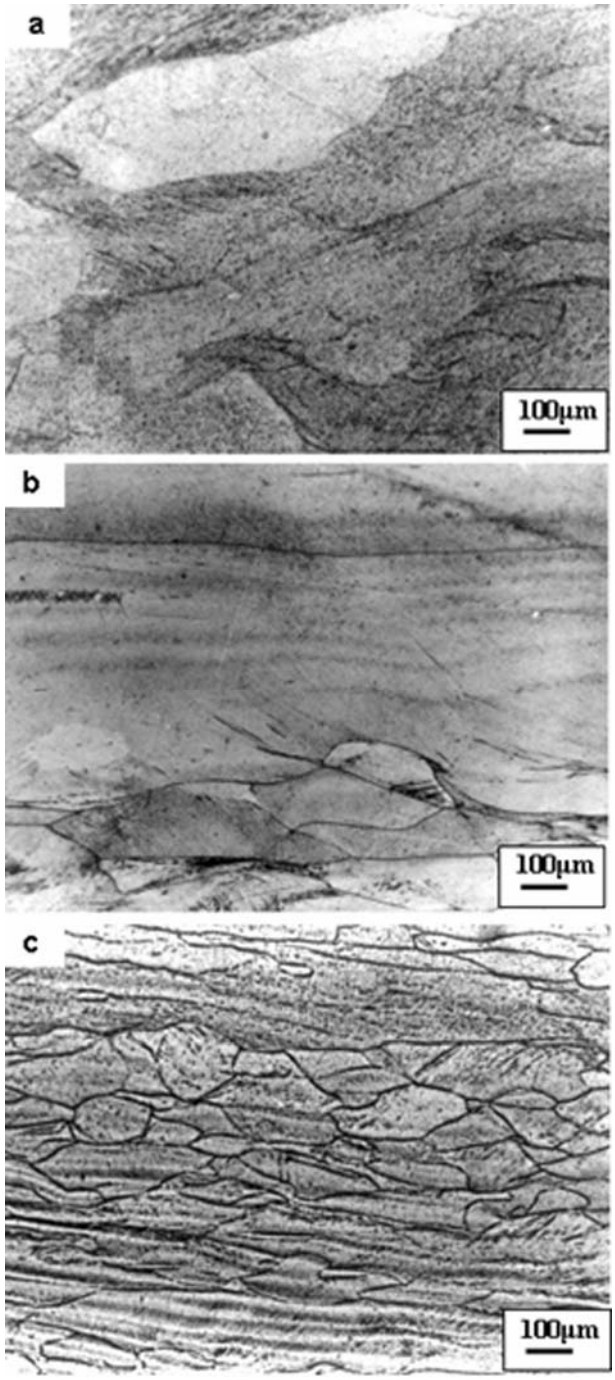

Figure 4. Optical microstructures of 80% hot-rolled alloys: (**a**) Ti–8Nb, (**b**) Ti–12Nb and (**c**) Ti–16Nb.

The BSE microstructures of the alloys in the β ST condition are shown in figure 7. The WQ specimens exhibit a typical martensitic microstructure. Very fine platelet-type features indicative of martensitic transformation are seen inside the prior β grains. The bright field (BF) TEM micrograph also reveals the presence of α'' phase with platelet-type features (figure 8a). The corresponding SAD pattern of the α'' phase is shown in figure 8b. The size of martensitic platelets decreases with increase in Nb content which is in agreement with that of martensitic microstructures of Ti-Mo alloys wherein the martensitic plates become finer with increase in Mo content (Davis *et al* 1979).

The XRD studies show the presence of α'' (orthorhombic) in alloy Ti–8Nb and α'' and ω phases in alloys Ti–12Nb and Ti–16Nb (figure 9). Based on the X-ray peak intensities of α'' and ω phases, it can be inferred that the volume fraction of ω is quite small as compared to that of α'' phase and it increases with the increase in Nb content. The lattice parameters of the constituent phases in all alloys in the β STWQ conditions are given in table 5. A comparison of the lattice parameters of α'' phase indicates that the *b*/*a* ratio decreases with increase in Nb concentration, while the *c* parameter remains nearly constant. The observed change in the *b*/*a* ratio is in agreement with the results obtained by Brown *et al* (1964). The *c*/*a* ratio of the ω phase in alloys Ti–12Nb and Ti–16Nb are 0·614 and 0·612, respectively. It has been suggested that *c*/*a* ratio of this phase is always 0.613, irrespective of the alloying additions (Hickman 1968, 1969a, b). The *c*/*a* ratios of the alloys in the present investigation are quite close to 0·613. The minor deviation of *c*/*a* ratio from 0·613 observed in the present study can be attributed to the presence of a small volume fraction of the ω phase resulting in only a few non-overlapping peaks with very low intensities.

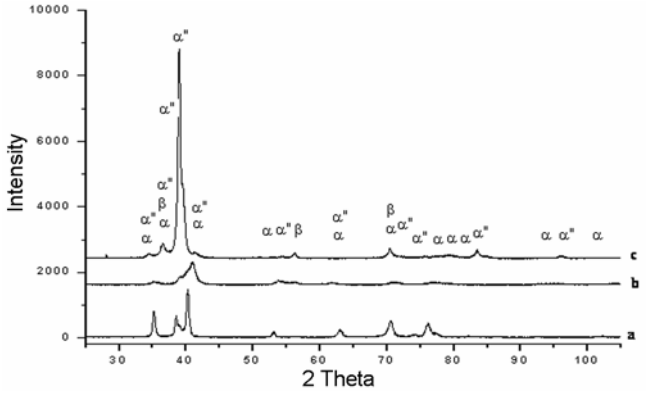

Figure 5. XRD patterns of hot-rolled alloys: (a) Ti–8Nb, (b) Ti–12Nb and (c) Ti–16Nb.

Table 3. Phases observed by XRD and their lattice constants in experimental alloys in 80% hot-rolled specimens.

Alloy	Phase(s)	Lattice constant (Å)		
		a	*b*	*c*
Ti–8Nb	α	2·953(5)	–	4·686(5)
	β	3·262(0)	–	–
Ti–12Nb	α''	3·054(8)	5·085(4)	4·616(6)
	β	3·264(0)	–	–
Ti–16Nb	α''	3·170(5)	4·969(2)	4·628(9)
	β	3·268(0)	–	–

Two different types of martensitic structures i.e. α' (hexagonal) and α'' (orthorhombic) are reported in titanium alloys depending upon the content of β alloying elements (Brown *et al* 1964; Young *et al* 1974; Sugimoto *et al* 1980; Collings 1984; Singh *et al* 1990; Boyer *et al* 1994; Geetha *et al* 2001, 2004). The critical composition limits of the β alloying elements in binary Ti–X (X = Nb, Mo, Ta, W, etc) for the formation of α'' have been reported in literature (Collings 1984; Boyer *et al* 1994). The α'/α'' boundary in the binary Ti–Nb system is around 5·7 atom%. The formation of the orthorhombic α'' phase in the present investigation after β ST WQ is therefore not surprising due to the presence of Nb contents which are higher than the critical limit. Banumathy *et al* (2009) recently studied the structure of α'' phase using Rietveld refinement of XRD data of these alloys. They have shown that formation of α'' phase occurs since Ti/Nb atoms are not able to reach hexagonal positions during WQ. This breaks the hexagonal symmetry and results in formation of α'' (orthorhombic) phase. It is to be noted that the space group of α'' phase is a subgroup of both the α and β phases.

As mentioned above, the alloys Ti–12Nb and Ti–16Nb exhibits the α'' and ω phases in β STWQ condition. The ω precipitation titanium alloys occurs in two distinct modes (Hickman 1968, 1969; Duerig *et al* 1980; Collings 1984). In relatively dilute alloy compositions, the ω phase forms during rapid quenching from the β phase field to a temperature below the ω start temperature (t_ω). This is referred to as athermal ω. The mechanism of the formation of athermal ω has been discussed earlier (Hickman 1968, 1969; Collings 1984). The ω phase also forms during aging of β-quenched alloys as well as in alloys richer in β alloying elements. This is called isothermal ω (Hickman 1968, 1969; Duerig *et al* 1980; Collings 1984).

It has been reported that a narrow composition range exists with the overlapping boundary of the martensitic and $\beta + \omega$ phase field, in which ω appears athermally during rapid quenching from the β phase field. Therefore, the presence of athermal ω phase in the β STWQ condition in the present study indicates two possibilities. In the first case, the alloy forms three phases viz. α'', β and ω after quenching and it is difficult to detect small amount of β phase by XRD technique due to low intensity and

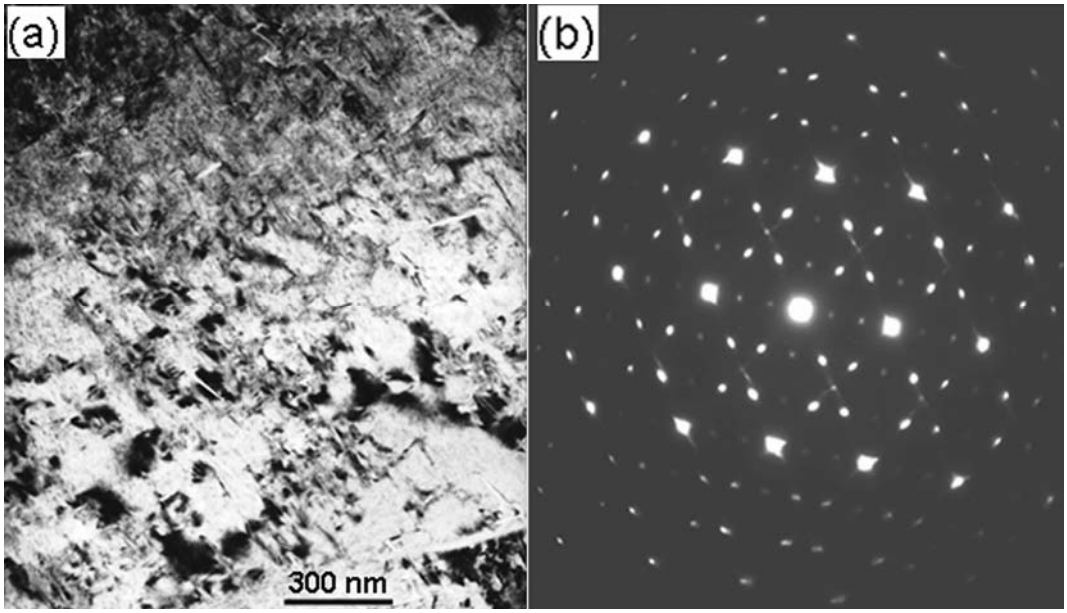

Figure 6. TEM microstructure of hot-rolled Ti–16Nb alloy: (**a**) BF and (**b**) diffraction pattern: [110] β zone superimposed with [1120]ω and [2110]ω zones.

Table 4. β and $\alpha + \beta$ heat treatment details for the experimental alloys.

Sl. No	Heat treatment	Designation	Observed phases by XRD		
			Ti–8Nb	Ti–12Nb	Ti–16Nb
1	950°C, 30 min + WQ	β STWQ	α''	α'', ω	α'', ω
2	β STWQ + 350°C/24 h + AC	β STWQ A1	α	α, α'', β, ω	α'', β, ω
3	β STWQ + 450°C/24 h + AC	β STWQ A2	α, β	α, α'', β, ω	α, α'', β, ω
4	β STWQ + 550°C/24 h + AC	β STWQ A3	α, β	α, β	α, β
5	950°C, 30 min + FC	β STFC	α, β, ω	α, β, ω	α, β, ω
6	680°C, 1 h + WQ	$\alpha + \beta$ STWQ	α, β, ω	α, α'', β, ω	α, α'', β, ω
7	$\alpha + \beta$ STWQ + 350°C/24 h + AC	$\alpha + \beta$ STWQ A1	α, β, ω	α, β, ω	α, β, ω
8	$\alpha + \beta$ STWQ + 450°C/24 h + AC	$\alpha + \beta$ STWQ A2	α, β	α, β	α, β
9	$\alpha + \beta$ STWQ + 550°C/24 h + AC	$\alpha + \beta$ STWQ A3	α, β	α, β	α, β
10	680, 1 h + FC	$\alpha + \beta$ STFC	α, β, ω	α, β, ω	α, β, ω

overlapping peaks. It is important to mention here that the first non-overlapping peak of the β phase lies at 2θ equal to 55·54° corresponding to {200} reflection which is very close to $\{20\bar{2}1\}$ peak of ω phase. In the other case, the alloy consists of two different regions i.e. Nb lean and Nb rich due to micro segregation. Figure 7d indicates the presence of micro segregation in Ti–12Nb and Ti–16Nb alloys. The Nb lean regions transform to α'' martensitic phase while Nb rich regions probably go down into narrow composition range as mentioned above and it transforms to ω phase after quenching.

Moffat and Larbalestier (1988) studied the competition between the martensitic and ω phases in alloys 20–70 atom% Nb as a function of quench rate and alloy composition. They have observed that as the temperature of β phase alloys decreases, the instability of *bcc* lattice increases. The α'' and ω phases compete to form in a sufficiently unstable lattice. The mode of β phase decomposition is determined by quench rate. The formation of α'' phase is favoured by fast quenching rate in alloys of 25 atom% Nb or less. The α'' phase is not observed in alloys with high Nb contents. The ω phase is preferred by slow quench rate. High Nb (60–70 atom%) stabilizes a single β phase microstructure.

It has been argued that both the $\beta \rightarrow \alpha''$ and $\beta \rightarrow \omega$ transformation are thermodynamically allowed over a wide range of alloy compositions (Moffat and Larbalestier 1988). It shows that the favoured transformation is determined by kinetics. The quench rate also determines the extent of diffusion possible during a quench, which may alter the athermal nature of $\beta \rightarrow \omega$ transformation. Moffat and Larbalestier (1988) observed both the α'' and ω phases in 25 atom% Nb alloy and attributed this to the fast quench rate at the perimeter of the specimen resulting

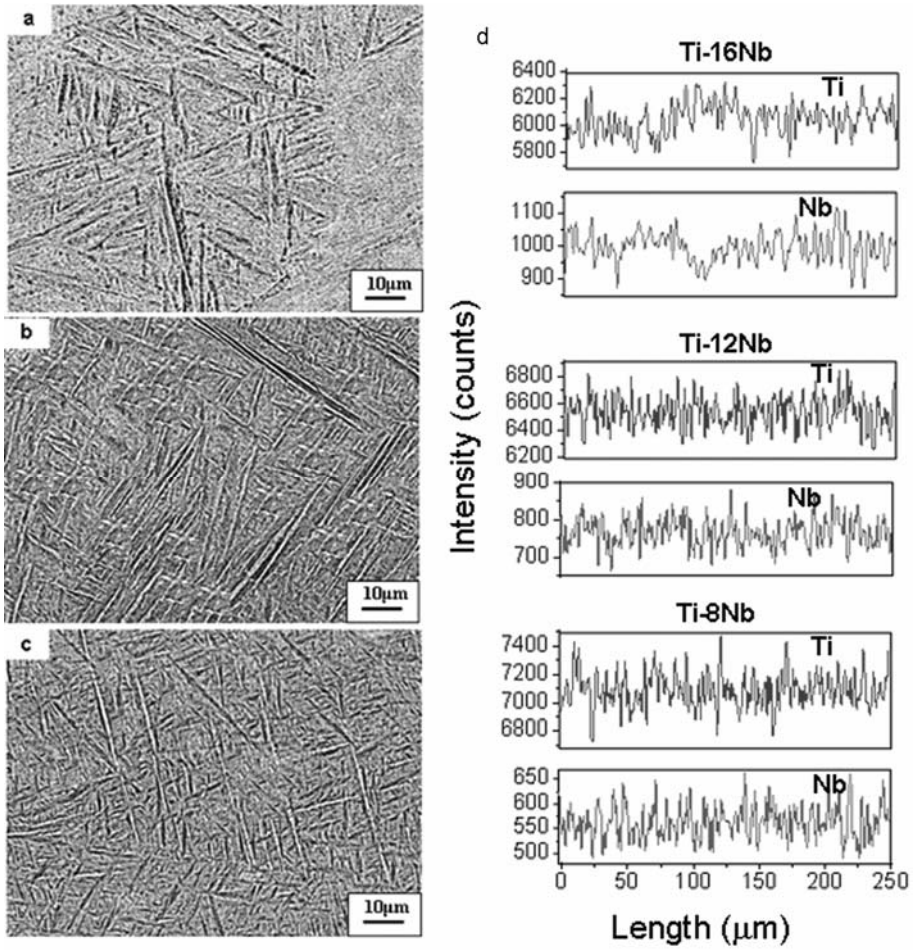

Figure 7. BSE microstructures of β solution treated (950°C, 30 min and WQ) alloys: (**a**) Ti–8Nb, (**b**) Ti–12Nb (**c**) Ti–16Nb and (**d**) elemental profile of Ti and Nb.

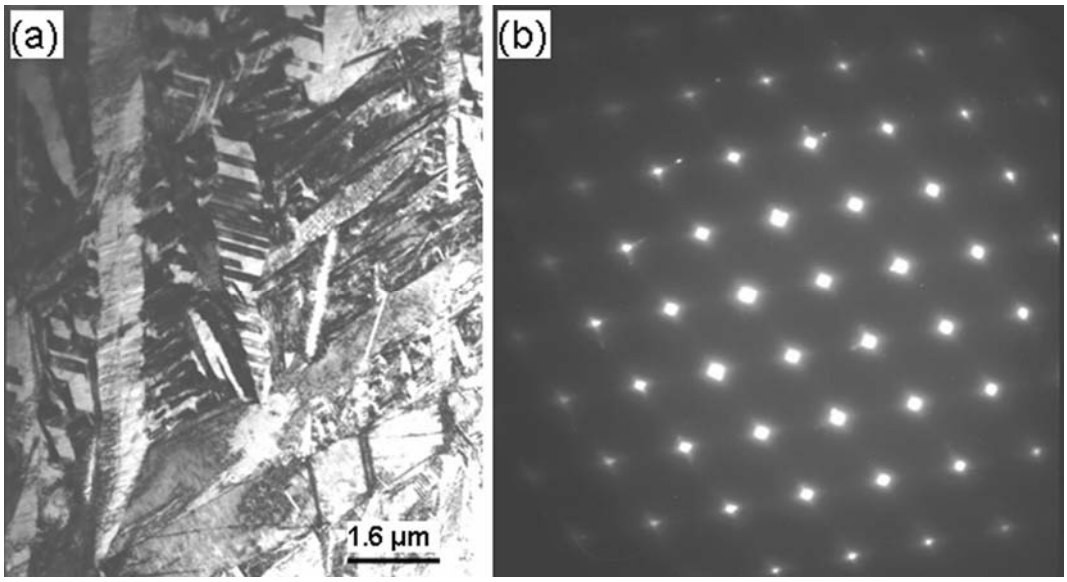

Figure 8. TEM microstructure of alloy Ti–16Nb in β STWQ condition: (**a**) BF and (**b**) SAD pattern of α'' phase with [002] zone axes.

Table 5. Lattice constants of constituent phases in β heat-treated alloys.

		Ti–8Nb alloy (Å)			Ti–12Nb alloy (Å)			Ti–16Nb alloy (Å)		
HT	Phase(s)	*a*	*b*	*c*	*a*	*b*	*c*	*a*	*b*	*c*
β STWQ	α''	2·980(0)	5·0762(5)	4·694(9)	3·059(0)	5·087(0)	4·703(0)	3·107(0)	5·014(0)	4·696(0)
	ω	–	–	–	4·613(9)	–	2·834(1)	4·614(5)	–	2·826(1)
β STFC	α	2·948(1)	–	4·684(3)	2·950(1)	–	4·683(8)	2·949(0)		4·685(2)
	β	3·278(5)	–	–	3·279(6)	–	–	3·284(3)	–	–
	ω	4·613(2)	–	2·816(0)	4·615(3)	–	2·813(8)	4·608(1)	–	2·826(6)
β STWQ + A1	α''	–	–	–	3·054(2)	5·054(0)	4·711(9)	3·099(4)	4·976(3)	4·709(4)
	α	2·968(7)	–	4·695(4)	2·949(8)	–	4·681(4)	–	–	–
	β	–	–	–	3·273(3)	–	–	3·292(0)	–	–
	ω	–	–	–	4·617(3)	–	2·834(8)	4·623(6)	–	2·818(9)
β STWQ + A2	α''	–	–	–	3·054(1)	5·053(1)	4·700(6)	3·097(4)	5·012(7)	4·697(9)
	α	2·966(5)	–	4·701(9)	2·952(6)	–	4·683(2)	2·956(5)	–	4·690(7)
	β	3·284(1)	–	–	3·282(5)	–	–	3·287(6)	–	–
	ω	–	–	–	4·611(6)	–	2·836(8)	4·614(6)	–	2·831(1)
β STWQ + A3	α	2·962(0)	–	4·704(4)	2·961(2)	–	4·691(6)	2·967(1)	–	4·690(8)
	β	3·296(9)	–	–	3·300(8)	–	–	3·295(5)	–	–

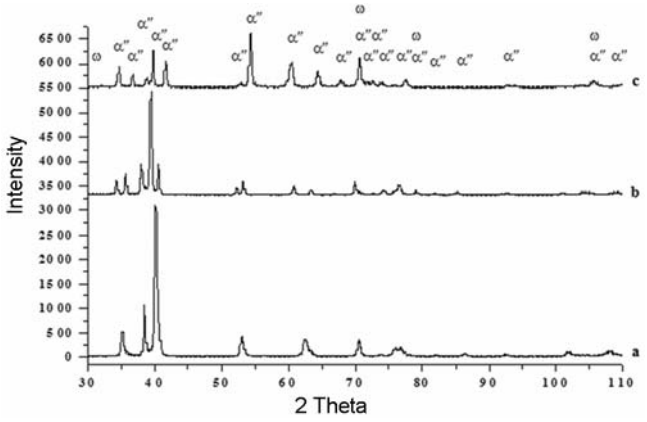

Figure 9. XRD patterns of β solution treated (950°C, 30 min and WQ) alloys: (a) Ti–8Nb, (b) Ti–12Nb and (c) Ti–16Nb.

in α'' phase while at the centre, it was slow enough to facilitate the formation of ω precipitate.

The β STFC specimens show a basket weave type microstructure (figure 10). The size of α platelets decreases with increase in Nb concentration. The Ti–16Nb alloy exhibits a cris-cross type of microstructure with fine plates. XRD studies reveal the presence of α, β and ω phases in all the three alloys (figure 11). The intensity of β phase peaks increases with increase in Nb content. This indicates that the volume fraction of the β phase increases since Nb is a β stabilizer. The lattice parameters of the constituent phases in β STFC condition are given in table 5. The lattice parameters of α phase remain nearly the same in all alloys while the lattice parameter of the β phase increases with increase in Nb content. The *c*/*a* ratio of ω phase remains very close to 0·613 as mentioned above (Hickman 1968, 1969; Davis *et al* 1979). The ω phase observed in the β STFC condition is different than that of athermal ω seen in β STWQ condition. It appears that the β phase is getting enriched due to preferential partitioning of Nb during furnace cooling. The elemental profiles exhibit the presence of micro segregations of Ti and Nb atoms (figure 10d). This shifts the overall composition of the β phase to $\omega + \beta$ phase field (Collings 1984; Boyer *et al* 1994) which results in ω and β phases after furnace cooling.

3.3b $\alpha + \beta$ *heat treatments*: The details of $\alpha + \beta$ heat treatments and the corresponding observed phases are given in table 4. It is to be noted that the solution treatment temperature (680°C) lies within $\alpha + \beta$ phase field for both the alloys Ti–8Nb and Ti–12Nb while for the alloy Ti–16Nb, it is very close to β transus temperature. BSE micrographs of the $\alpha + \beta$ STWQ are given in figure 12 which reveal a very fine microstructure for all the three alloys. BSE microstructure of the alloy Ti–8Nb (figure 12a) exhibits α platelets (α_p) in transformed β regions. The alloy, Ti–12Nb, consists of very fine platelets while the alloy, Ti–16Nb, exhibits transformed β with interior short and elongated α. TEM BF micrograph of the alloy Ti–16Nb reveals fine microstructure (figure 13). The ω phase is finely distributed inside the α and α'' plates.

The XRD studies of $\alpha + \beta$ STWQ specimens reveal the presence of α, β and ω phases in alloy Ti–8Nb and α, α'', β and ω phases in both the alloys Ti–12Nb and Ti–16Nb (table 4). The lattice parameters of all the observed phases are given in table 6. It appears that during $\alpha + \beta$ heat treatment of the alloy Ti–8Nb, α and β phases are getting enriched by Ti and Nb, respectively due to

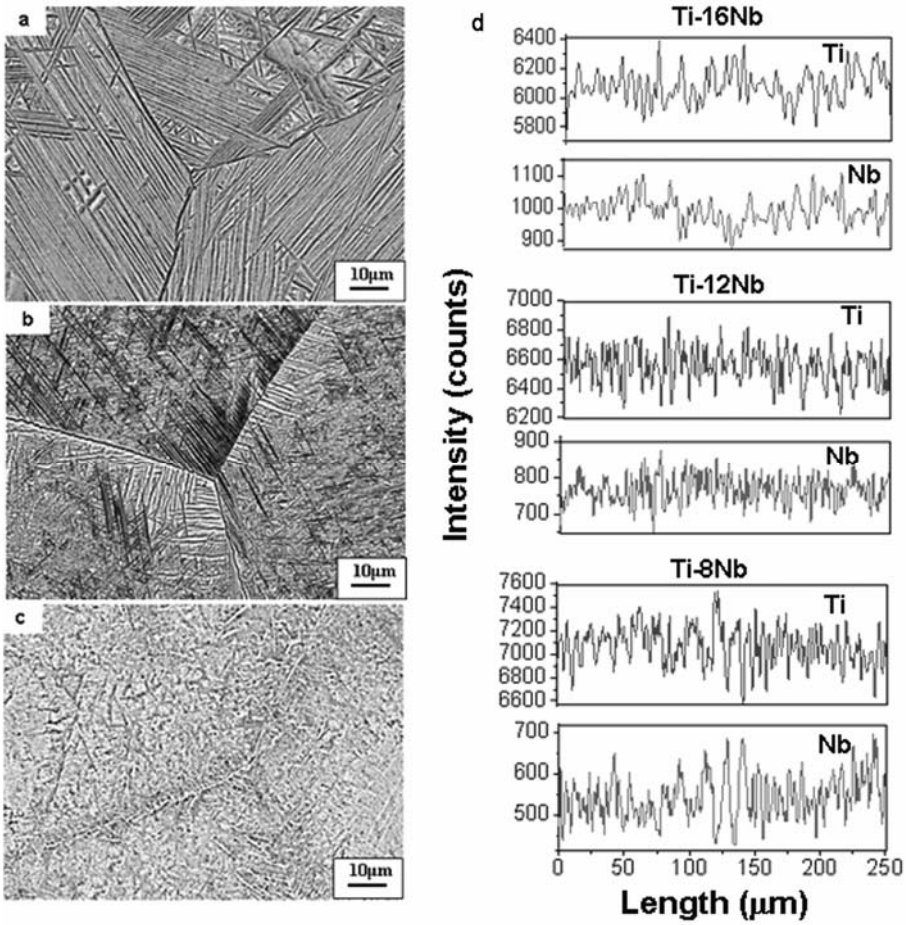

Figure 10. BSE microstructures of β solution treated (950°C, 30 min and FC) alloys: (**a**) Ti–8Nb, (**b**) Ti–12Nb, (**c**) Ti–16Nb and (**d**) elemental profile of Ti and Nb.

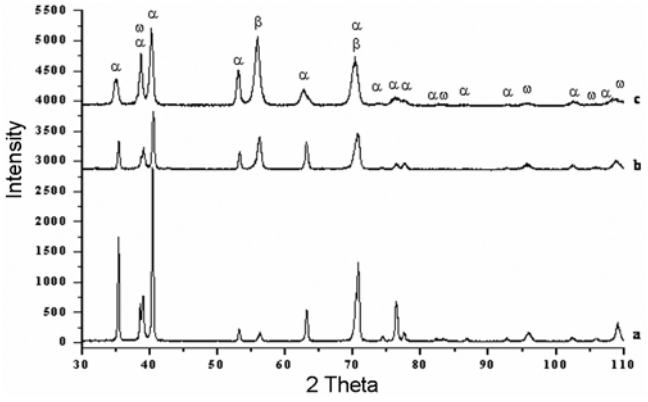

Figure 11. XRD patterns of β solution treated (950°C, 30 min and FC) alloys: (a) Ti–8Nb, (b) Ti–12Nb and (c) Ti–16Nb.

partitioning effect (figure 12). As a result, it shifts the composition of Nb enriched phase to $\alpha'' + \omega + \beta$ phase field (Collings 1984; Boyer *et al* 1994). The absence of α'' phase in this specimen can, therefore, be probably attributed to the small volume fraction of α'' phase, which cannot be detected by XRD due to low intensity and overlapping of peaks.

The evolution of the phases in alloys Ti–12Nb and Ti–16Nb is similar to that of the alloy Ti–8Nb. The increase in Nb content increases the volume fraction of β phase in $\alpha + \beta$ phase field at 680°C. In this case too, the alloy concentration lies in three-phase field i.e. $\alpha'' + \beta + \omega$ as mentioned above (Collings 1984) thereby resulting in the formation of α, α'', β and ω phases after the $\alpha + \beta$ STWQ heat treatment.

The microstructures of the experimental alloys in the $\alpha + \beta$ STFC condition are shown in figure 14. The FC specimens reveal the presence of a two-phase microstructure although the morphologies of the phases in three alloys are quite different. A comparison of WQ and FC microstructures shows that the volume fraction of the α phase increases with decreasing cooling rates. The XRD studies of $\alpha + \beta$ STFC specimens reveal the presence of α, β and ω phases. The lattice parameters of these phases are given in table 6. On slow cooling from $\alpha + \beta$ ST, there is an enrichment of phase in Nb (figure 14) which shifts the β phase composition to $\omega + \beta$ phase field

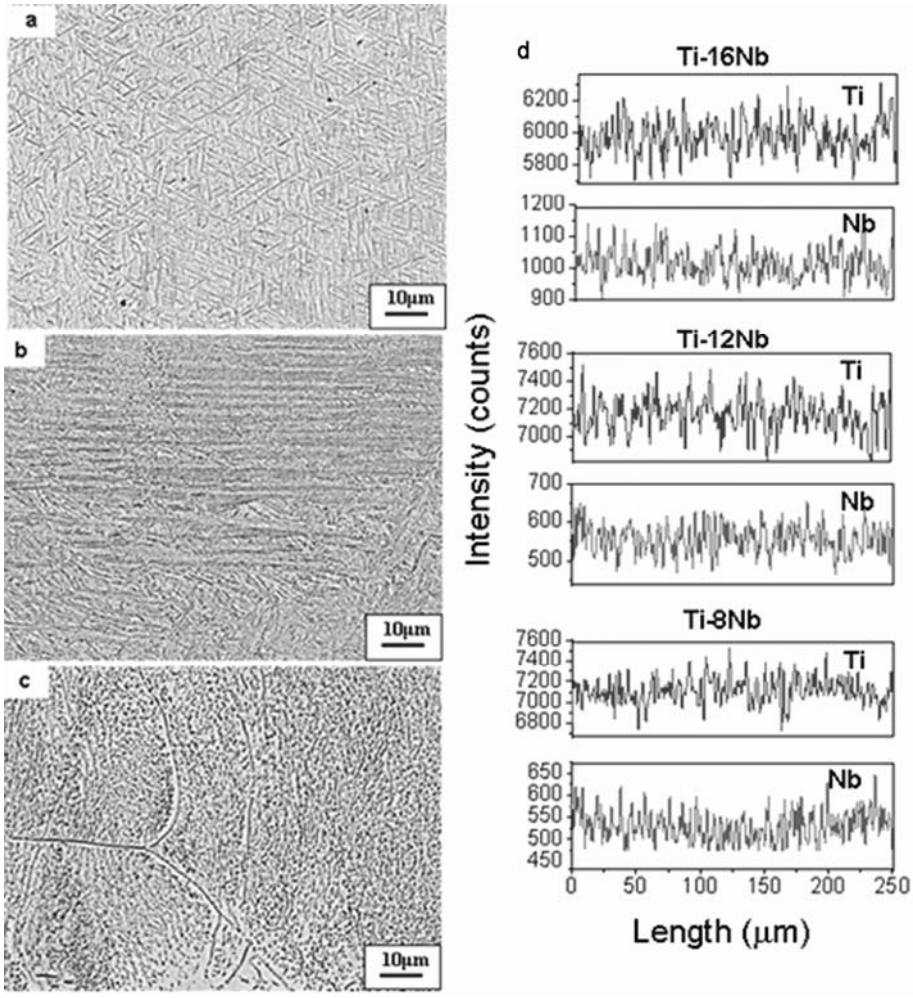

Figure 12. BSE microstructures of $\alpha + \beta$ solution treated (680°C, 1 h and WQ) alloys: (**a**) Ti–8Nb, (**b**) Ti–12Nb, (**c**) Ti–16Nb and (**d**) elemental profile of Ti and Nb.

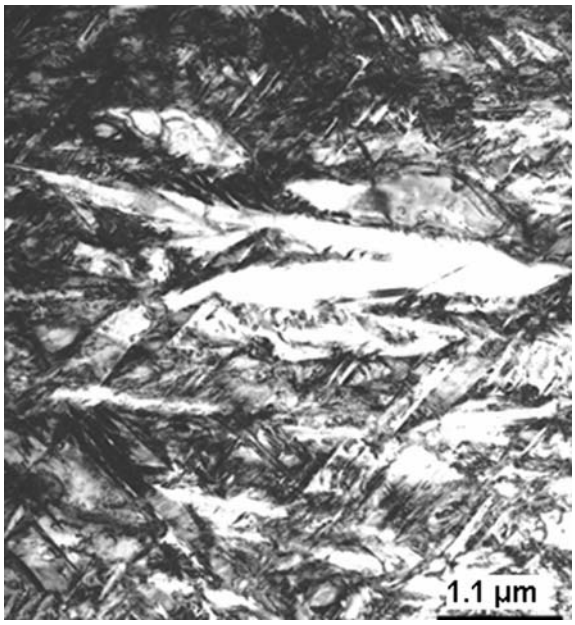

Figure 13. BF TEM micrograph of alloy Ti–16Nb in $\alpha + \beta$ STWQ condition.

(Collings 1984). As a result, $\alpha + \beta$ STFC heat treatment results in α, β and ω phases in all the three alloys.

3.4 *Aging treatments*

The aging treatments have been carried out at three different temperatures, viz. 350, 450 and 550°C for solution treated and WQ specimens. All the samples have been air cooled after aging.

3.4a *β solution treatment*: The β WQ specimen shows a gradual change in the microstructure with increasing aging temperatures. The WQ specimen of the alloy Ti–8Nb displays platelets of martensitic phase (figure 15). The aging at 350°C reduces the sharpness of the martensitic plates and also introduces a globular morphology. The aging at 450°C has clearly resulted in coarse α plates (figure 15). Further increase in aging temperature (550°C) leads to the formation of thicker α plates. These α plates consist of fine parallel plates inside having newly nucleated α plates.

Table 6. Lattice constants of constituent phases in $\alpha + \beta$ heat treated alloys.

		Ti–8Nb alloy (Å)			Ti–12Nb alloy (Å)			Ti–16Nb alloy (Å)		
HT	Phase	*a*	*b*	*c*	*a*	*b*	*c*	*a*	*b*	*c*
($\alpha + \beta$) STWQ	α''	–	–	–	3·004(6)	4·970(9)	4·748(1)	3·089(4)	4·904(8)	4·692(0)
	α	2·954(9)	–	4·692(9)	2·951(1)	–	4·689(3)	2·950(8)	–	4·655(6)
	β	3·275(6)	–	–	3·278(7)	–	–	3·282(7)	–	–
	ω	4·614(2)	–	2·827(9)	4·620(5)	–	2·820(6)	4·586(0)	–	2·819(9)
($\alpha + \beta$) STFC	α	2·942(0)	–	4·674(8)	2·943(5)	–	4·683(0)	2·944(5)	–	4·685(6)
	β	3·270(9)	–	–	3·281(3)	–	–	3·286(8)	–	–
	ω	4·599(9)	–	2·809(8)	4·590(1)	–	2·824(5)	4·624(8)	–	2·821(8)
($\alpha + \beta$)	α	2·952(4)	–	4·688(7)	2·958(6)	–	4·683(1)	2·957(7)	–	4·685(3)
STWQ + A1	β	3·272(5)	–	–	3·274(2)	–	–	3·276(6)	–	–
	ω	4·597(5)	–	2·825(1)	4·610(0)	–	2·816(1)	4·620(4)	–	2·822(4)
($\alpha + \beta$)	α	2·952(3)	–	4·691(0)	2·953(0)	–	4·692(9)	2·955(2)	–	4·694(3)
STWQ + A2	β	3·274(4)	–	–	3·275(6)	–	–	3·278(7)	–	–
	ω	–	–	–	–	–	–	4·626(5)	–	2·817(8)
($\alpha + \beta$)	α	2·954(5)	–	4·686(9)	2·958(8)	–	4·685(2)	2·959(8)	–	4·666(7)
STWQ + A3	β	3·277(3)	–	–	3·281(7)	–	–	3·287(3)	–	–
	ω	–	–	–	–	–	–	4·629(3)	–	2·838(6)

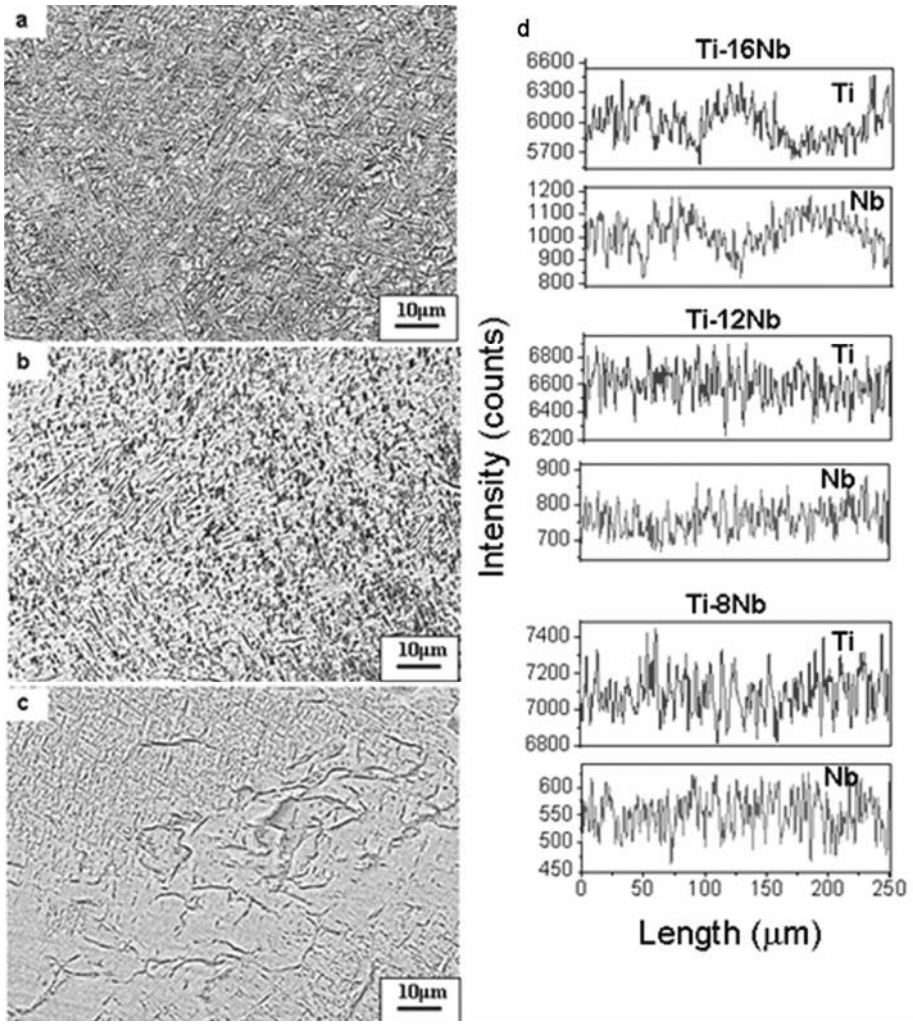

Figure 14. BSE SEM microstructures of $\alpha + \beta$ solution treated (680°C, 1 h and FC) alloys: (**a**) Ti–8Nb, (**b**) Ti–12Nb, (**c**) Ti–16Nb and (**d**) elemental profile of Ti and Nb.

The alloy Ti–8Nb in β STWQ condition consists of α'' only. The aging of WQ specimen at 350°C results in α while aging at 450 and 550°C shows the presence of α and β phases (table 4). The lattice parameters of the α phase of aged specimens are nearly the same while the lattice parameter of the β phase slightly increases. It can be seen that a and c parameters of the aged specimens are higher than those of β STFC specimen. This can be attributed to a composition change of α phase in β STFC specimens due to the presence of β and ω phases.

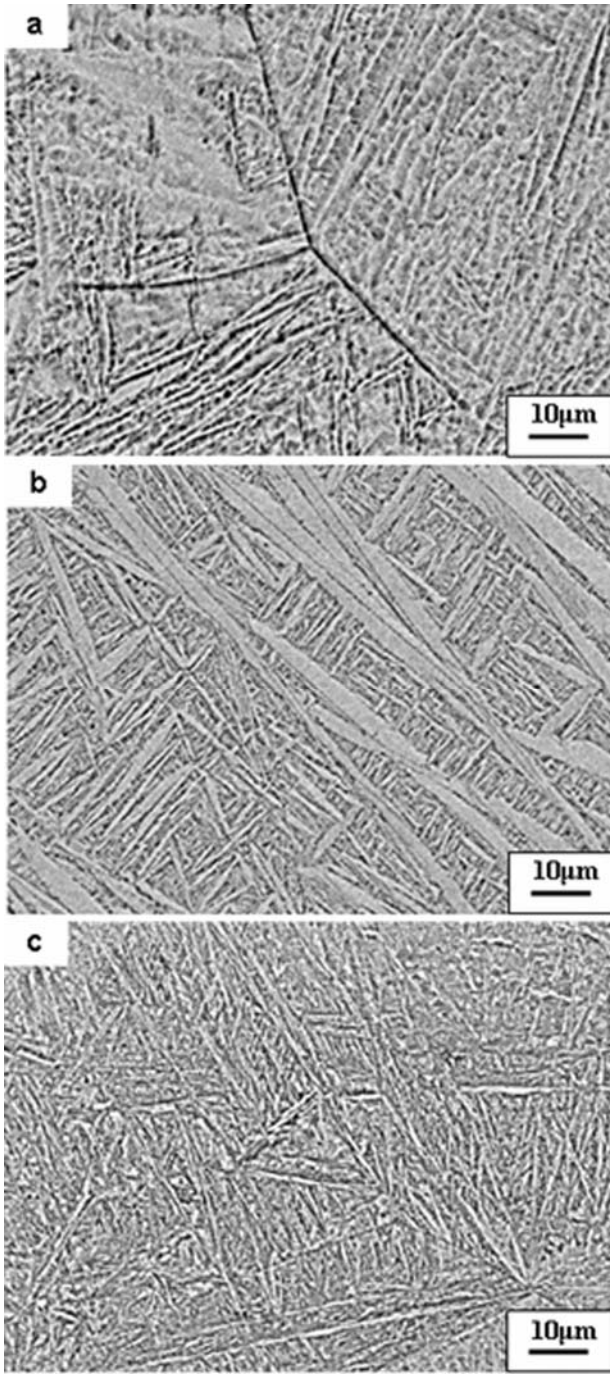

Figure 15. BSE SEM microstructures of β solution treated (950°C, 30 min and WQ) and aged at 450°C, 24 h and AC (A2) alloys: (**a**) Ti–8Nb, (**b**) Ti–12Nb and (**c**) Ti–16Nb.

The presence of α phase clearly indicates that α'' martensitic phase has completely transformed to the α phase at 350°C aging. It is important to mention that orthorhombic martensitic α'' phase can transform to $\alpha+\beta$ ($M_s >$ room temperature) or β ($M_s =$ room temperature), where M_s is the martensitic start temperature (Murakami 1980). The presence of α phase in 350°C aged specimen indicates two possibilities: (i) transformation of α'' to α phase and (ii) aging temperature is inappropriate for formation of enough β phase to be detected by XRD technique.

A transformation of the α'' to α phase without β precipitation as observed in 350°C aged specimen has been reported (Young *et al* 1974). It has been observed that the α'' phase transforms through precipitation of α needles rather than that of β particles. Singh *et al* (1993) reported the transformation of α'' to α' by aging at a stabilizing treatment temperature (530°C, 6 h) without any precipitation of β phase. In the case of the alloy Ti–8Nb, it appears that α'' phase transforms to α or α and β phases during aging depending on aging temperatures.

Aging β WQST of the alloy Ti–12Nb reduces the sharpness of the edge of α plates, increases the size, introduces globularization and exhibits newly nucleated α plates aligned parallel within the large α plates. The 550°C aged microstructure of the alloy Ti–12Nb exhibits platelet structure. The platelet structure is absent in alloy Ti–16Nb and aging has introduced fine microstructure.

The aging of β STWQ specimens of the alloy Ti–12Nb results in α, α'', β and ω phases at 350 and 450°C and α and β phases at 550°C (table 4). The alloy Ti–16Nb consists of α'', β, ω, α'', α, β, ω, α, β phases in 350, 450 and 550°C aged specimens, respectively (table 4). The lattice parameters of the constituent phases are given in table 5. The lattice parameters of α'' phases remain nearly constant in comparison to those of β STWQ specimen. The lattice parameter of α and β phases exhibits its highest value in case of 550°C aged specimens as compared to those of β STFC and other aged specimens. This can again be attributed to partitioning of alloying elements in α and β phases only. The c/a ratios of the ω phase remain very close to 0·613 in all aging temperatures (Hickman 1968, 1969a, b).

The alloy Ti–12Nb exhibits α'' and ω phases in the β STWQ condition. As mentioned above, the martensitic α'' phase observed in the β STWQ condition is unstable and can transform to α and $\alpha+\beta$ phases. The presence of α'' phase in aged specimens of the alloy Ti–12Nb at 350 and 450°C is probably due to only partial transformation of the α'' phase to α and β phases. Further increase in aging temperature (550°C) results in complete transformation of α'' phase to α and β phases and ω to α phase, thereby the aged microstructure consists of α and β phases only.

The behaviour of Ti–16Nb alloy during aging is also the same except that the 350°C aged specimen exhibit α'', β and ω phases (table 4). The absence of α phase (unlike the alloy Ti–12Nb) in this specimen can probably be attributed to the small volume fraction of α phase which cannot be detected by XRD due to low intensity and also overlapping peaks. Further, increase in aging temperature (450°C) exhibits α, α'', β and ω phases (similar to the alloy Ti–12Nb) and finally, aging at 550°C results in α and β phases.

Balcerzak and Sass (1972) studied the formation of ω phase in as-quenched and aged specimens of Ti–Nb alloys ranging from 18 to 40-atom% Nb. They have observed an equiaxed ω phase in as-quenched specimens. The continuous aging has increased the size of the particles and evolved into an ellipsoidal shape. The competition between α and ω phases in metastable β matrix has been studied during isothermal aging by Moffat and Larbalestier (1988). It has been shown that the aging temperature is the key factor that determines which phase will precipitate first in the quenched specimen. Aging at temperatures below 400°C results in extensive ω phase precipitation while at high temperatures ($\geq$ 400°C), exhibits α precipitation. The ω phase is metastable with respect to α phase. The α phase nucleates independently on existing ω precipitate and grows at the expense of the ω precipitate.

The aging behaviour of the present alloys in the quenched condition is quite different than those of the above-mentioned alloys. The quenched alloys consist of α' or α'' and ω phases depending on the Nb concentration unlike the metastable β phase. The aging at low temperature initially transforms α' phase to α and β phases and ω forms from β phase. On the other hand, aging at higher temperatures (550°C) transforms existing ω phase to α phase. Since ω phase is associated with high hardness and brittleness, low temperature aging at which the ω phase formed is generally not carried out in titanium alloys (Duerig *et al* 1980). However, presence of ω phase can help in achieving fine distribution of α phase on subsequent aging or heat treatment at slightly higher temperatures (Silcock 1958).

3.4b *$\alpha + \beta$ solution treatment*: Aging of $\alpha + \beta$ STWQ specimens at 350°C does not introduce significant changes in the microstructures. However, fine scale microstructural changes may be occurring in the transformed β phase, which can only be observed by TEM. Aging at 450°C further refines the microstructures due to fine precipitation of α phase (figure 16). Further increase in aging temperature (550°C) introduces slightly coarse microstructures than those of 450°C aged specimens.

XRD studies of the aged specimens reveal the presence of α, β and ω phases at 350°C in all the three alloys (table 4). Further increase in aging temperature (450 and 550°C) shows the presence of α and β phases. It appears that increase in aging temperature from 350 to 450°C has introduced fine α precipitates in the microstructure due to $\omega \rightarrow \alpha$ transformation. As a result, 450°C aged specimens consist of a very fine microstructure. It is very difficult to conclude anything about the transformation of α'' to α or $\alpha + \beta$ in the present study since some amount of β phase is already present in as quenched specimens. The

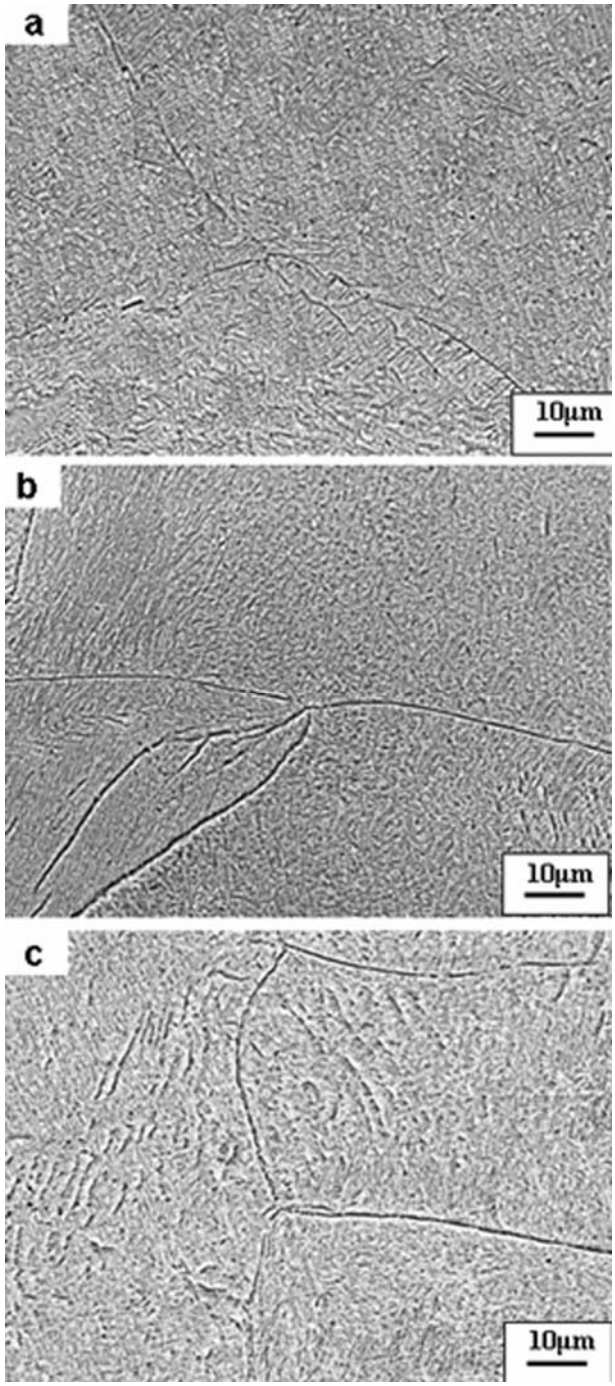

Figure 16. BSE SEM microstructures of $\alpha + \beta$ solution treated (680°C, 1 h and WQ) and aged at 450°C, 24 h and AC (A2) alloys: (**a**) Ti–8Nb, (**b**) Ti–12Nb and (**c**) Ti–16Nb.

presence of α and β phases in all the alloys in the 550°C aged specimens indicates that only coarsening of existing phase occurs during aging.

The lattice parameters of all the phases in the $\alpha+\beta$ STWQ are given in table 6. The lattice parameters of the α phase remains nearly constant in the aged specimens. The *c*/*a* ratio of ω phase is very close to 0·613. There is a slight increase in the lattice parameter of β phase with increase in aging temperature, which can be attributed to the change in composition during aging.

4 Conclusions

(I) The alloy Ti–8Nb exhibits α and β phases while the alloys Ti–12Nb and Ti–16Nb show the presence of α'' and β phases in the as-cast and hot-rolled conditions. The presence of α'' phase in the as-cast and hot-rolled specimens can be attributed to high Nb content.
(II) The alloy Ti–8Nb shows α'' phase and the alloys Ti–12Nb and Ti–16Nb exhibit α'' and ω phases in β STWQ condition. The ω phase observed in latter two alloys is due the presence of high Nb concentration.
(III) The alloy Ti–8Nb shows the presence of α, β and ω phases while the alloys Ti–12Nb and Ti–16Nb exhibit α, α', β and ω phases in $\alpha+\beta$ STWQ condition.
(IV) High temperature aging results in α and β phases.
(V) All the three alloys exhibit the presence of α, β and ω phases in β STFC and $\alpha+\beta$ STFC conditions.
(VI) The presence of ω phase in the solution-treated condition depends on cooling rate and Nb content while in aged specimens depends on aging temperature as well as Nb concentration.

Acknowledgements

(AKS) and (SB) are grateful to the Ministry of Defence, Government of India, for financial support. We are grateful to Dr G Malakondaiah, Director, Defence Metallurgical Research Laboratory (DMRL), Hyderabad for his encouragement and support. We extend our thanks to Dr T K Nandy for many fruitful discussions.

References

Balcerzak A T and Sass S L 1972 *Metall. Trans.* **3** 1601
Banumathy S, Mandal R K and Singh A K 2009 *J. Appl. Phys.* **106** 093518
Brown A R G, Clark D, Eastabrook J and Jepson K S 1964 *Nature* **201** 914
Boyer R, Welsch G and Collings E W 1994 *Titanium alloys, materials properties handbook* (Materials Park, OH: ASM International)
Collings E W 1984 *Physical metallurgy of titanium alloys* (OH: American Society of Metals)
Davis R, Flower H M and West D R F 1979 *J. Mater. Sci.* **14** 712
Duerig T W, Terlinde G T and Williams J C 1980 *Titanium 80. Science and Technology* (eds) H Kimura and O Izumi (New York: The Metals Society—American Institute of Mining, Metallurgical and Petroleum) **2**, 1299
Eylon D, Fujishiro S, Postans P J and Froes F H 1984 *J. Met.* **1** 55
Geetha M, Singh A K, Muraleedharan K, Gogia A K and Asokamani R 2001 *J. Alloys and Compds.* **329** 264
Geetha M, Singh A K, Gogia A K and Asokamani R 2004 *J. Alloys Compds* **384** 131
Hickman B S 1968 *J. Inst. Met.* **96** 330
Hickman B S 1969a *J. Mater Sci.* **4** 554
Hickman B S 1969b *Trans. Metall. Soc. AIME* **245** 1329
Jepson K S, Brown A R G and Gray J A 1970 *The science and application of titanium: Proc. first int. conf. on titanium* (eds) R I Jaffee and W E Promisel (London: Pergamon Press) pp. 677–690
Lagaree K 1989–1993 PKSFAReg, U.S. Patent, Registered Version 2.04, PKWARE Inc.
Moffat D L and Larbalestier D C 1988 *Metall. Trans.* **A19** 1677, 1687
Murakami Y 1980 *Titanium 80. Sci. and Technol.* **1** 153
Murray J L 1987 *Phase diagrams of binary titanium alloys* (Metals Park, Ohio: ASM International) pp. 188–194
Silcock J M 1958 *Acta Metall.* **6** 481
Singh A K, Ramachandra C, Tavafoghi M and Singh V 1993 *J. Mater. Sci. Lett.* **129** 697
Sugimoto T, Komatsu S, Kamei K, Yoshida H and Murakami Y 1980 *Titanium 80, Science and technology* (eds) H Kimura and O Izumi (New York: The Metals Society—American Institute of Mining, Metallurgical and Petroleum) **4**, pp. 2981–2990
Young M, Levine E and Margolin H 1974 *Met. Trans.* **5** 1891